PRELIMINARY RESULTS ON THE MEASUREMENT OF THE RATIO $\sigma(\nu_\mu e \to \nu_\mu e)/\sigma(\bar{\nu}_\mu e \to \bar{\nu}_\mu e)$

CHARM Collaboration

J.V. Allaby, U. Amaldi, G. Barbiellini, L. Barone, A. Capone,
W. Flegel, W. Kozanecki, K.H. Mess, M. Metcalf, J. Meyer, R.S. Orr,
J. Panman, A.M. Wetherell, K. Winter
CERN, Geneva, Switzerland

J. Aspiazu, V. Blobel, F.W. Büsser, H. Daumann, P.D. Gall,
H. Grote, B. Kröger, E. Metz, F. Niebergall, K.H. Ranitzsch,
P. Stähelin
II. Institut für Experimentalphysik, Univ. Hamburg, Hamburg, Germany

F. Bergsma, J. Dorenbosch, M. Jonker, C. Nieuwenhuis, F. Udo
NIKHEF, Amsterdam, The Netherlands

A. Baroncelli, B. Borgia, C. Bosio, F. Ferroni, E. Longo,
P. Monacelli, F. de Notaristefani, P. Pistilli, C. Santoni,
L. Tortora, V. Valente
INFN, Rome, Italy

P. Gorbunov, E. Grigoriev, V. Kaftanov, V. Khovansky, A. Rosanov
ITEP, Moscow, U.S.S.R.

Presented by C. Santoni

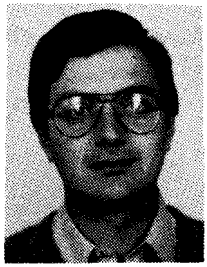

ABSTRACT

A description of the method of analysis is given and preliminary results are presented on the measurement of the ratio of neutrino-electron to antineutrino-electron cross-sections using a fine-grain calorimeter.

1. INTRODUCTION

The main goal of pursuing the study of neutrino and antineutrino scattering on electrons is to determine the coupling constants of the leptonic weak neutral current and to compare them with the predictions of the gauge model, thus avoiding the uncertainties inherent in the use of hadronic targets.

In this paper we discuss: i) the performance of the CHARM apparatus in detecting $(\bar{\nu})_\mu e$ events; ii) the measurement of the antineutrino-electron cross-section; iii) preliminary results on the measurement of the ratio of neutrino to antineutrino cross-sections.

2. PERFORMANCE OF THE CHARM APPARATUS

The detector[1] is a fine-grain marble calorimeter followed by a muon spectrometer. The target calorimeter consists of 78 subunits. A subunit comprises a marble plate of 3×3 m^2 surface area and 8 cm thickness followed by two planes of sensitive elements: i) 128 proportional drift tubes, each tube having dimensions of $3 \times 3 \times 400$ cm^3, and ii) 20 plastic scintillators of dimensions $15 \times 3 \times \times 300$ cm^3 oriented at 90° with respect to the tubes. A subunit is one radiation length thick. The calorimeter measures the angle and the energy of the neutrino-induced showers. It is surrounded by a magnetized iron frame aimed at detecting low-energy muons and at improving the shower containment. The target calorimeter is followed by four toroidal iron magnets, each containing 75 cm of iron to detect muons produced in charged-current events. A partial schematic view of the apparatus is shown in Fig. 1.

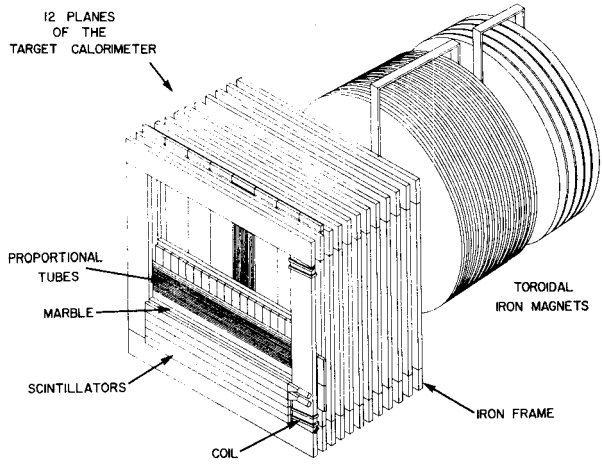

Fig. 1 Partial view of the fine-grain calorimeter and the muon spectrometer.

At present accelerator energies, the neutrino scattering processes are characterized by a cross-section proportional to the total energy and hence to the target mass. The cross-section for neutrino-electron scattering is expected to be four orders of magnitude smaller than the neutrino-nucleon cross-section. The first two experimental requirements for detecting $\nu_\mu e$ events are therefore: i) large target mass to collect enough statistics (in this experiment the fiducial mass is 80 tons); ii) good separation of electromagnetic events from hadronic events. In the CHARM calorimeter this separation is based essentially on the different widths of electromagnetic and hadronic showers. Figure 2 shows the distributions of the width of 20 GeV electron and pion-induced showers as measured by a) the scintillators and b) the proportional tubes; Γ is the width of a Cauchy distribution fitting the transversal profile of the central part of the shower, as measured by the scintillators; σ is the r.m.s. width of the shower profile measured in a larger fiducial area by the proportional tubes. To select electron-induced showers we require: $\Gamma < 1.6$ cm and $\sigma < 9$ cm. The efficiency of this selection for electron-induced showers is (85 ± 5%), whilst the rejection of pion-induced showers is larger than 99% [2]. A further distinction between electrons and pions is based on the difference between the development of the showers close to the vertex. We require i) a single hit in the first tube plane following the vertex, and ii) an energy deposition in the first scintillator plane of the shower (E_{first}) in the range 3-50 MeV, i.e. larger than ½ and smaller than ∿ 8 minimum ionizing particles (m.i.p.). For electrons, the efficiency of these cuts combined with those on the shower width was measured to be (61 ± 9)% [2].

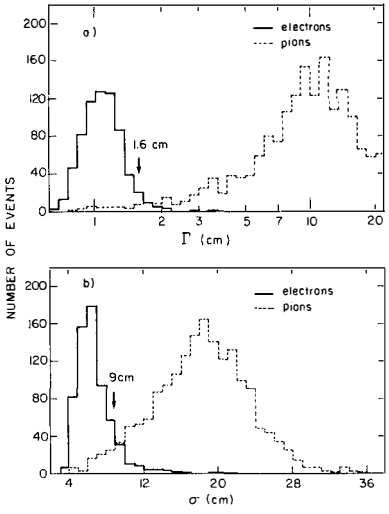

Fig. 2 Distributions of the width of 20 GeV electron and pion showers; a) as measured by the scintillators, and b) as measured by the proportional tubes. The width parameters Γ and σ are discussed in the text.

The detector was exposed to the horn-focused wide-band neutrino and antineutrino beams of the CERN 400 GeV Super Proton Synchrotron (SPS). About 1.2×10^6 neutrino and 1.5×10^6 antineutrino interactions have been collected in the fiducial volume of the calorimeter. The candidate events are searched for among those which i) are muonless, ii) satisfy the selection criteria previously described, iii) have an angle θ with respect to the neutrino beam axis which is smaller than 100 mrad, and iv) have an energy deposited in the calorimeter in the range $7.5 \leq E \leq 30$ GeV. The good events are contaminated by a background due to two sources: a) elastic and quasi-elastic charged-current events induced by the ν_e and $\bar{\nu}_e$ contamination of the beam; b) semileptonic neutral-current events with a dominant electromagnetic component in the hadronic shower. At high energies in neutrino-electron scattering, the electron recoils at very small angles $\left[< (2\, m_e c^2/E)^{\frac{1}{2}} \approx 7 \text{ mrad}\right]$ with respect to the neutrino direction. The two backgrounds (a) and (b) have a broader angular distribution. This defines the third experimental requirement which has to be satisfied to measure neutrino-electron scattering: the angular resolution has to be of the order of a few milliradians.

The performance of the CHARM detector, as measured[2] in an electron beam, is summarized in Table 1.

Table 1

Projected angle and energy r.m.s. resolution for electromagnetic showers

Electron energy (GeV)	15	20	50
$\Delta\theta$ projection (mrad)	12	11	7
Energy resolution (%)	5.0	4.5	2.8

The neutrino and antineutrino candidate events are plotted in Fig. 3a and 3b versus the variable $E^2\theta^2$. We have chosen this variable because it emphasizes the different kinematics of the signal with respect to the backgrounds. The measured angular resolution implies that 90% of the good events have $E^2\theta^2 \leq 0.12$ GeV^2, corresponding to the first two bins of Fig. 3. To subtract the background, we extrapolate from the region 0.12-0.54 GeV^2 to the region $E^2\theta^2 < 0.12$ GeV^2. The $E^2\theta^2$ distribution of background (a), known to be energy independent, has been experimentally determined[3] by using data on elastic and quasi-elastic charged-current reactions induced by muon neutrinos (antineutrinos). The $E^2\theta^2$ dependence of background (b) was determined by a Monte Carlo simulation using the known neutrino (antineutrino) energy spectrum and assuming that the Q^2 dependence of neutral-current events is the same as that of charged current ones. The normalization of backgrounds (a) and (b) was obtained by a study of the energy deposition in the first scintillator plane

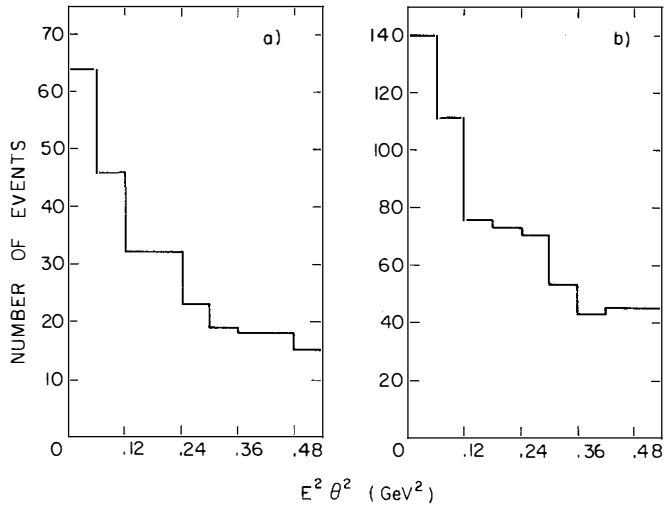

Fig. 3 Distributions of the candidate events versus the variable $E^2\theta^2$: a) neutrinos, b) antineutrinos.

following the shower vertex in the region $0.12 \leq E^2\theta^2 \leq 0.54$ GeV^2. This analysis is based on the observation that electromagnetic showers initiated by a π^0 produced by semileptonic neutral-current processes have an energy deposition in this scintillator corresponding mainly to an even number of m.i.p., whilst the events due to background (a) [as well as to $(\bar{\nu})_\mu$e scattering] give an energy deposition corresponding mainly to an odd number of m.i.p. Figure 4 shows the measured[2] E_{first}

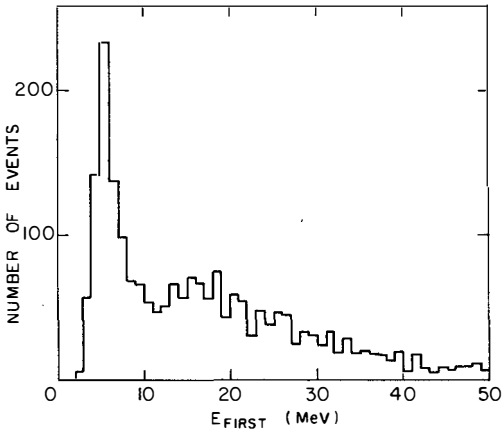

Fig. 4 15 GeV electrons. Distribution of the energy E_{first} deposited in the first scintillator plane of the shower.

distribution for 15 GeV electrons. In the region E_{first} = 3-9 MeV we observe ∿ 35% of all events. Figures 5 and 6 show the E_{first} distribution for the neutrino- and antineutrino-candidates in the regions $E^2\theta^2 < 0.12$ GeV^2 and $0.12 \leq E^2\theta^2 \leq 0.54$ GeV^2. The number of the events attributed to background (a) is compatible with the number of events with $E_{first} < 9$ MeV in the region $0.12 \leq E^2\theta^2 \leq 0.54$ GeV^2. In agreement with the computed $(\bar{\nu})_\mu e$ fluxes in the region 7.5-30 GeV, the contribution of reaction (a) to the background is much more important in the antineutrino case than in the neutrino one.

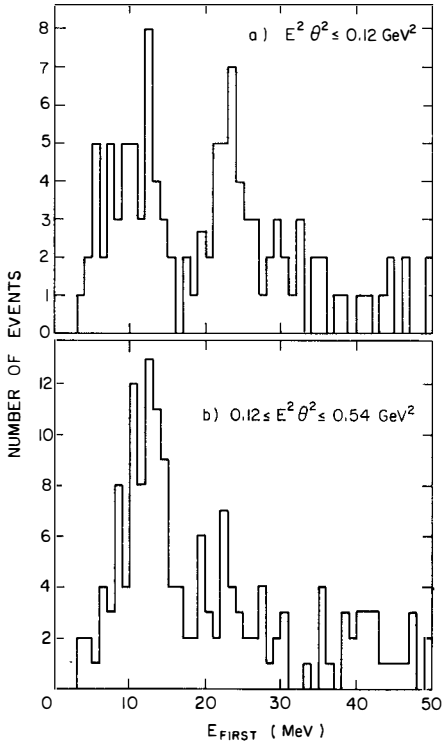

Fig. 5 Neutrino candidates. Distribution of the energy E_{first} deposited in the first scintillator plane of the shower: a) events with $E^2\theta^2 \leq 0.12$ GeV^2; b) events with $0.12 < E^2\theta^2 < 0.54$ GeV^2.

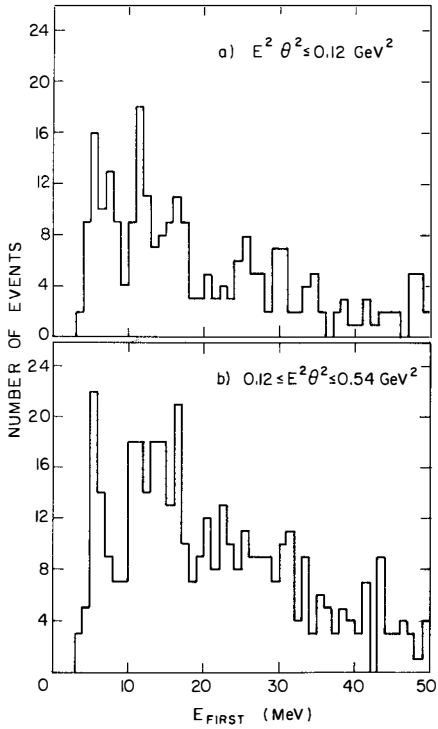

Fig. 6 Antineutrino candidates. Distribution of the energy E_{first} deposited in the first scintillator plane of the shower: a) events with $E^2\theta^2 \leq 0.12$ GeV^2; b) events with $0.12 \leq E^2\theta^2 \leq 0.54$ GeV^2.

3. RESULTS OF THE MEASUREMENT OF THE ANTINEUTRINO CROSS-SECTION

The previous method of analysis has led to a measurement of the antineutrino-electron cross-section[4] based on a sample corresponding to ∿ 80% of the full statistics. Out of ∿ 1.45×10^6 interactions obtained with 4.3×10^{18} 400 GeV protons on target, 537 candidates were selected by the criteria described above. The $E^2\theta^2$ distribution of these events is shown in Fig. 7a. The background subtraction procedure attributed 175 events to source (a), 282 events to source (b), and 72 ± 16 events to the signal. The E_{first} variable permits the selection of a clear "electron" sample of 120 events through the requirement $E_{first} < 9$ MeV corresponding to 1.5 m.i.p. These events have the $E^2\theta^2$ distribution shown in Fig. 7b. Out of them, 25 ± 7 are attributed to antineutrino-electron scattering. The signal is reduced by a factor of ∿ 3, in agreement with the measured efficiency (∿ 35%) for observing electromagnetic showers initiated by single electrons which deposit energy less than 1.5 m.i.p. in the first scintillator plane. At the same time the background is reduced by a factor of ∿ 10. Assuming a y distribution as predicted by the standard model, the 72 ± 16 events correspond to a cross-section

$$\sigma\left(\bar{\nu}_\mu e\right)/E_{\bar{\nu}} = \left[1.70 \pm 0.33(\text{stat}) \pm 0.39(\text{syst})\right] \times 10^{-42} \text{ cm}^2/\text{GeV} .$$

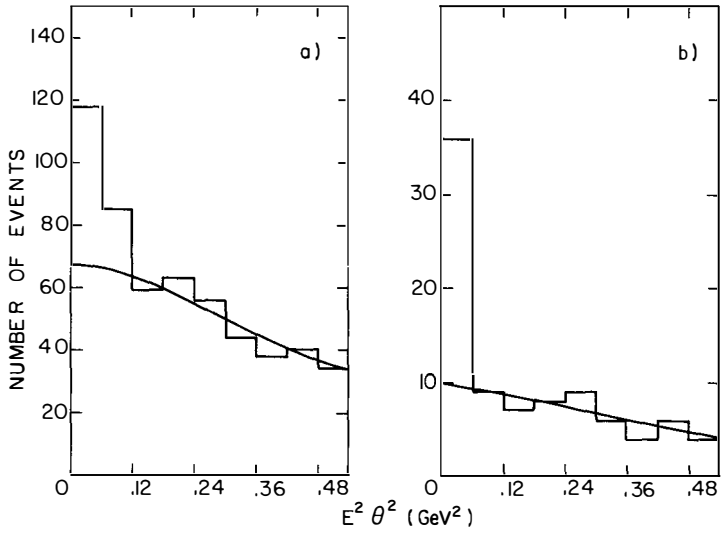

Fig. 7 Distributions of the antineutrino candidate events versus the variable $E^2\theta^2$(80% of full stat.): a) events satisfying the selection criteria discussed in the text; b) subset of sample (a) satisfying the criterion $E_{first} < 9$ MeV. The background subtraction is discussed in the text.

The normalization to the number of incoming antineutrinos was done by making use of the known[5] antineutrino-nucleon total cross-section $[0.41\ E\nu \times 10^{-38}\ (cm^2/GeV)]$ and by measuring the number of antineutrino and neutrino interactions in the same fiducial volume of the calorimeter. The measured cross-section agrees with the prediction of the Glashow-Salam-Weinberg model for

$$\sin^2\theta = 0.29 \pm 0.05\ (stat)\ .$$

The present result agrees, within the still large statistical and systematic errors, with what has been found in previous experiments on purely leptonic weak interactions.

4. THE RATIO OF NEUTRINO TO ANTINEUTRINO CROSS-SECTIONS

The most general expressions for the neutrino and antineutrino-electron scattering cross-sections are[6]

$$\sigma^{\nu} = \frac{G^2 m_e E\nu}{2\pi}\,\beta^2\left[(C_V - C_A)^2 + \frac{1}{3}(C_V + C_A)^2\right]$$

$$\sigma^{\bar{\nu}} = \frac{G^2 m_e E\nu}{2\pi}\,\beta^2\left[\frac{1}{3}(C_V - C_A)^2 + (C_V + C_A)^2\right]$$

C_V and C_A are the vector and the axial coupling constants. In the standard model we have $C_V = \frac{1}{2} - 2\sin^2\theta$ and $C_A = -\frac{1}{2}$; β^2 is a multiplying factor related to the isospin of Higgs particles. Assuming a doublet structure of Higgs mesons, this factor is equal to 1. It follows that the most direct measurement of the parameter $\sin^2\theta$ is achieved by measuring the cross-section ratio without any hypothesis on the structure of the Higgs sector. In Fig. 8 the value of $R = \sigma(\nu_\mu e)/\sigma(\bar{\nu}_\mu e)$ is plotted versus the value of $\sin^2\theta$; R varies rapidly when $\sin^2\theta$ is in the range 0.1-0.3. In particular $(\Delta \sin^2\theta/\sin^2\theta) = \frac{1}{2}(\Delta R/R)$. This fact

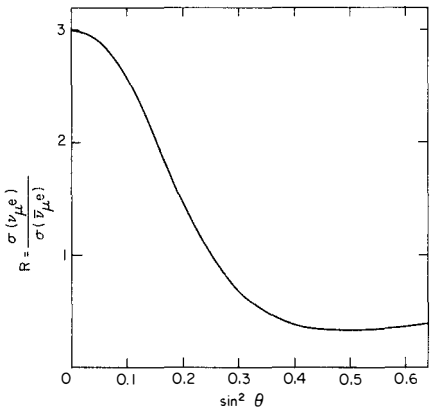

Fig. 8 Ratio of neutrino-electron to antineutrino-electron cross-sections versus $\sin^2\theta$.

allows a more accurate measurement of $\sin^2\theta$ in purely leptonic process. From an experimental point of view, the deviation of $\sin^2\theta$ from the ratio of two cross-sections measured with the same apparatus gives a result which is less subject to systematic errors than the deviation of $\sin^2\theta$ from measurements of the absolute values of the two cross-sections. Table 2 gives a comparison of the estimates of the three main systematic errors of two approaches: i) of the antineutrino cross-section[4], ii) measurement of the ratio R of the two cross-sections.

Table 2

Comparison of the systematic uncertainties of the σ and R methods

Systematic error	$\sigma\bar{\nu}_\mu$ (%)	R (%)
Background subtraction	20	12
Detection efficiency of electrons	15	0
Normalization	6	5
Over-all systematic error	26	13

The error in the background subtraction is reduced because, even if the contributions are different, the sources are the same. The uncertainty in the efficiency to select $(\bar{\nu})_\mu e$ candidates drops out. In the ratio measurement the beam fluxes are monitored in two ways: i) by measuring the ratio of the neutrino and antineutrino interactions on nucleons and by making use of the known ratio of neutrino to antineutrino total cross-section; and, ii) by measuring the number of single μ^- (μ^+), induced by quasi-elastic ν_μ ($\bar{\nu}_\mu$)-nucleon interaction and by making use of the equality of the cross-sections for exclusive and small-y neutrino- and antineutrino-nucleon interactions on an isoscalar target. In conclusion, the ratio method is less affected by systematic errors than the cross-section method and is also less sensitive to theoretical uncertainties. This measurement is therefore a promising new approach to the fundamental problem of measuring the weak mixing angle in purely leptonic processes and of verifying the universality of coupling to leptons and quarks. The final analysis of the ratio measurement, based on $\sim$ 40 neutrino-electron events and on $\sim$ 80 antineutrino-electron events collected by the CHARM Collaboration, is still in progress.

REFERENCES

1) A.N. Diddens et al. (CHARM Collab.), Nucl. Instrum. Methods 178 (1980) 27.

2) M. Jonker et al. (CHARM Collab.), CERN-EP/82-08.

3) M. Jonker et al. (CHARM Collab.), Phys. Lett. 93B (1980) 203.

4) M. Jonker et al. (CHARM Collab.), Phys. Lett. 105B (1981) 242.

5) M. Jonker et al. (CHARM Collab.), Phys. Lett. 99B (1981) 265.

6) D.A. Ross and M. Veltman, Nucl. Phys. B95 (1975) 135.